Yeast formin Bni1p has multiple localization regions that function in polarized growth and spindle orientation

Wenyu Liu, Felipe H. Santiago-Tirado, and Anthony Bretscher
Department of Molecular Biology and Genetics, Weill Institute for Molecular and Cell Biology, Cornell University, Ithaca, NY 14853

ABSTRACT **Formins are conserved proteins that assemble unbranched actin filaments in a regulated, localized manner. Budding yeast's two formins, Bni1p and Bnr1p, assemble actin cables necessary for polarized cell growth and organelle segregation. Here we define four regions in Bni1p that contribute to its localization to the bud and at the bud neck. The first (residues 1–333) requires dimerization for its localization and encompasses the Rho-binding domain. The second (residues 334–821) covers the Diaphanous inhibitory–dimerization–coiled coil domains, and the third is the Spa2p-binding domain. The fourth region encompasses the formin homology 1–formin homology 2–COOH region of the protein. These four regions can each localize to the bud cortex and bud neck at the right stage of the cell cycle independent of both F-actin and endogenous Bni1p. The first three regions contribute cumulatively to the proper localization of Bni1p, as revealed by the effects of progressive loss of these regions on the actin cytoskeleton and fidelity of spindle orientation. The fourth region contributes to the localization of Bni1p in tiny budded cells. Expression of mislocalized Bni1p constructs has a dominant-negative effect on both growth and nuclear segregation due to mislocalized actin assembly. These results define an unexpected complexity in the mechanism of formin localization and function.**

Monitoring Editor
Kerry S. Bloom
University of North Carolina

Received: Jul 20, 2011
Revised: Nov 23, 2011
Accepted: Nov 30, 2011

INTRODUCTION

The ability to polarize is a universal feature of eukaryotic cells that allows them to grow and divide, move, transport nutrients across epithelia, and so on. To probe the general mechanisms underlying cell polarity, we exploit the budding yeast *Saccharomyces cerevisiae* as an experimentally accessible model to study polarized growth and organelle segregation during the cell cycle. During bud growth, polarized actin cables are assembled that guide the transport of secretory vesicles for cell growth, as well as the segregation of organelles, all of which depend on transport by the myosin-V motor Myo2p (Pruyne *et al.*, 2004b). The polarized actin cables are nucleated and elongated by localized formins.

Formins are a family of conserved proteins that assemble unbranched actin filaments. They have been implicated in the formation of multiple cellular structures such as stress fibers, filopodia, cell–cell junctions, phagocytic cups, and contractile rings (Chesarone *et al.*, 2010). In budding yeast, there are two formin proteins, Bni1p and Bnr1p, which have different localizations and contribute to different sets of actin cables (Pruyne *et al.*, 2004a). During bud growth, Bni1p localizes dynamically to the bud tip, where it nucleates the assembly of cables, and later it is found at the bud neck, where it contributes to assembly of the contractile ring prior to cytokinesis, whereas Bnr1p is stably associated with the bud neck to generate cables extending into the mother cell (Pruyne *et al.*, 2004a; Buttery *et al.*, 2007). Although single deletion of either *BNI1* or *BNR1* is viable, deleting both is lethal (Vallen *et al.*, 2000; Ozaki-Kuroda *et al.*, 2001). All formins possess the defining domain formin homology 2 (FH2), generally in the C-terminal half of the molecule. Studies with the FH2 domain of Bni1p were the first to show that formins can nucleate the assembly of unbranched actin filaments and then remain associated with the elongating barbed end of the growing filaments (Pruyne *et al.*, 2002; Sagot *et al.*, 2002). N-Terminal to the FH2 domain is the proline-rich formin homology 1 (FH1) domain, which binds to

This article was published online ahead of print in MBoC in Press (http://www.molbiolcell.org/cgi/doi/10.1091/mbc.E11-07-0631) on December 7, 2011.

Address correspondence to: Anthony Bretscher (apb5@cornell.edu).

Abbreviations used: CC, coiled coil; DD, dimerization domain; DID, Diaphanous inhibitory domain; FH1, formin homology domain 1; FH2, formin homology domain 2; GBD, GTPase-binding domain; SBD, Spa2p-binding domain.

profilin–actin to enhance the assembly rate at the FH2-associated actin filament end (Sagot *et al.*, 2002). As members in the Diaphanous-related formin subfamily, Bni1p and Bnr1p also have an N-terminal Diaphanous inhibitory domain (DID) domain, which has been suggested to bind the C-terminal Diaphanous autoregulatory domain (Li and Higgs, 2003, 2005; Wang *et al.*, 2009). This autoinhibitory interaction is relieved at least in part by binding of Rho GTPases to the GTPase-binding domain (GBD), which partially overlaps with the DID (Li and Higgs, 2003, 2005; Lammers *et al.*, 2005; Otomo *et al.*, 2005; Rose *et al.*, 2005; Nezami *et al.*, 2006; Seth *et al.*, 2006). Biochemical and structural analyses have shown that the N-terminal region of the formin mDia1 is dimerized through a dimerization domain (DD; Li and Higgs, 2005; Otomo *et al.*, 2005), which is also present in Bni1p. Bni1p contains a unique region, the Spa2p-binding domain (SBD), which binds to Spa2p and has been suggested to localize Bni1p (Fujiwara *et al.*, 1998). Spa2p is part of a 12S complex called the polarisome that also contains Pea2p and Bud6p (Sheu *et al.*, 1998; Shih *et al.*, 2005). Bud6p binds the C-terminal region of Bni1p to enhance actin assembly and contribute to spindle orientation (Fujiwara *et al.*, 1998; Moseley and Goode, 2005; Delgehyr *et al.*, 2008).

The nucleus is a critical organelle whose segregation during cell division is essential for growth. During cell division the nuclear membrane does not break down, so the nucleus must be accurately oriented and elongated relative to the bud neck in order for both the mother and the bud to each inherit one nucleus at the end of mitosis. This nuclear orientation and elongation depends on forces acting on cytoplasmic microtubules radiating from the spindle pole bodies embedded in the nuclear membrane. Early during bud formation, the nucleus is initially oriented by the class V myosin Myo2p, which links Kar9p to Bim1p on the plus end of cytoplasmic microtubules and transports them down actin cables toward the bud (Beach *et al.*, 2000; Yin *et al.*, 2000; Hwang *et al.*, 2003). Because this step requires actin cables nucleated by Bni1p, *bni1* mutants have nuclear movement and microtubule orientation defects (Fujiwara *et al.*, 1999; Lee *et al.*, 1999; Theesfeld *et al.*, 1999). Later during anaphase, the elongation of the nucleus depends on the microtubule motor protein Dyn1p and associated dynactin complex (Li *et al.*, 1993; Muhua *et al.*, 1994). Thus nuclear movement is mediated by two pathways: one through Kar9p/Myo2p/Bni1p, and the other through Dyn1p and components of the dynactin complex. Failure of either pathway is not lethal and results in minor abnormalities in nuclear segregation; however, loss of both can be lethal (Fujiwara *et al.*, 1999; Miller *et al.*, 1999; Tong *et al.*, 2001).

In this study, we dissect Bni1p to define four independent localization regions in the protein. These regions contribute cumulatively to the appropriate localization of Bni1p to influence polarized growth and spindle orientation. We also show that Bni1p constructs that do not localize appropriately have a dominant phenotype that slows growth and interferes with spindle orientation due to the inappropriate assembly of mislocalized actin.

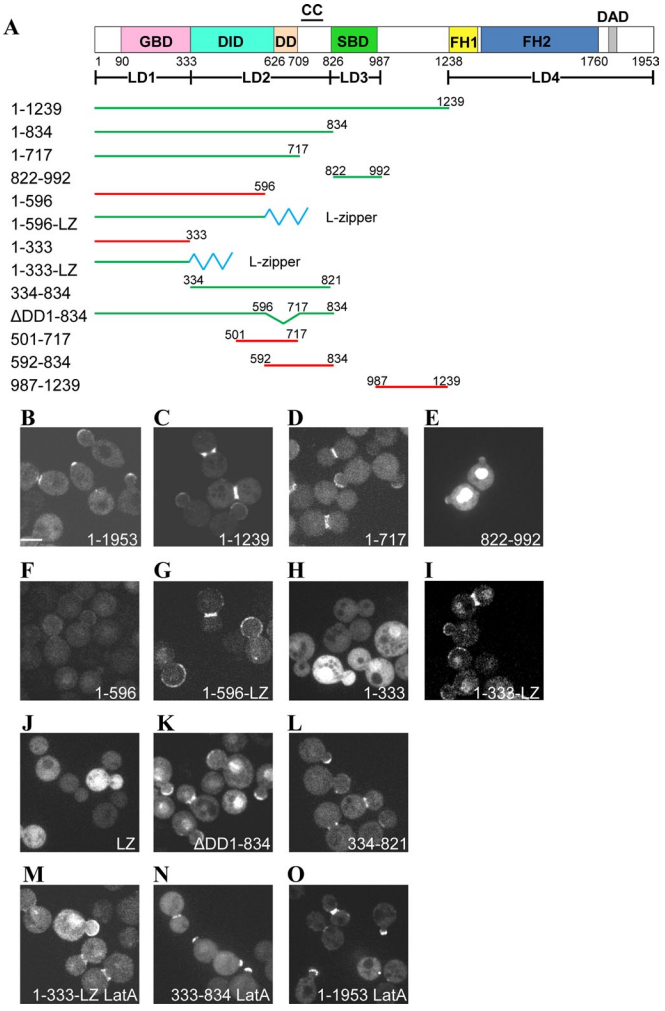

FIGURE 1: The N-terminal region of Bni1p has three localization domains. (A) Schematic diagram of Bni1p domains based on homology to mDia1, and the constructs examined. Constructs that localized to the bud cortex and bud neck during the right stages of the cell cycle are shown in green, whereas constructs that did not localize are shown in red. CC, predicted coiled coil; DAD, Diaphanous-autoinhibitory domain; DID, Diaphanous inhibitory domain; DD, dimerization domain; FH1, formin homology domain 1; FH2, formin homology domain 2; GBD, GTPase-binding domain; SBD, Spa2p-binding domain. (B–O) GFP images of cells overexpressing Bni1p N-terminal constructs in a *bni1*Δ background. Bni1p constructs were tagged with GFP at the C-terminus with expression from the *GAL1* promoter on a CEN plasmid. Cells were examined after 3–4 h induction with galactose. (M–O) GFP images of cells overexpressing the Bni1p N-terminal regions in a *bni1*Δ background after treatment with 200 μM latrunculin A for 10 min. Scale bar, 5 μm.

RESULTS

The N-terminal domain of Bni1p contains more than one localization region

It was shown that the N-terminal 1–1240 amino acids of Bni1p are sufficient for its localization (Ozaki-Kuroda *et al.*, 2001). To see whether a smaller piece of Bni1p can still localize appropriately, we expressed, using a *GAL1* promoter on a CEN plasmid, a series of C-terminally green fluorescent protein (GFP)–tagged constructs encompassing decreasing regions of the N-terminal domain to narrow down localization determinants. We designed the pieces to be expressed based on homology to structurally defined domains of mDia1 (Otomo *et al.*, 2005; Nezami *et al.*, 2006; Figure 1A). The constructs were expressed in both *bni1*Δ (Figure 1, B–O) and *BNI1* (Supplemental Figure S1A) cells to test whether the localization regions depend on endogenous Bni1p. All constructs expressed proteins of the expected size (Supplemental Figure S1B). The localizations of different constructs described in the following sections are summarized in Table 1.

Full-length Bni1p-GFP localizes at the bud growth site (Figure 1B), concentrates at the bud tip of small-budded cells, distributes more broadly as a cap in medium-budded cells, disappears from the

Bni1p-GFP constructs	Bud tip localization	Crescent at bud cortex	Bud neck localization
Bni1p	+++	+	+++
1–1239	+++	++++++	+++
1–834	+++	+++++	+++
1–717	+++	+++++	+++
822–992 (LD3)	++	+	++
1–596	+	+	+
1–596-LZ	+++	+++++	+++
1–333	–	–	+
1–333-LZ (LD1)	+++	+++++	+++
334–821 (LD2)	+++	+++	+++
ΔDD 1–834	+++	+++	+++
501–717	–	–	–
592–834	–	–	–
987–1239	–	–	–

Numbers indicate Bni1p amino acid residues present in the constructs. A plus or minus indicates whether the construct was detected by live imaging at the indicated place. The number of plus signs indicates how frequently it was seen in a log-phase culture.

TABLE 1: Localization of Bni1p N-terminal overexpression constructs.

bud cortex of large-budded cells, and reappears at the bud neck prior to cytokinesis (Ozaki-Kuroda *et al.*, 2001; Pruyne *et al.*, 2004a). Live-cell imaging of the Bni1p–1-1239–GFP construct showed a broader crescent localization than full-length Bni1p at the bud cortex of small and medium-sized buds and also localized to the bud neck late in the cell cycle (Figure 1C). The shortest N-terminal region that localized to the bud cortex well was Bni1p–1-717–GFP (Figure 1D). Because the SBD lies outside this construct and the Bni1p–822-992–GFP construct covering the SBD localizes mostly to the nucleus but also weakly to the bud cortex and bud neck (Figure 1E), Bni1p has at least two localization domains in its N-terminal 1–1239 amino acid region. Constructs shorter than Bni1p–1-717–GFP localized very weakly, with barely detectable localization to the bud cortex and neck (Figure 1, F and H).

The GBD domain of Bni1p localizes to the bud cortex when dimerized

As indicated, Bni1p–1-717–GFP localizes to the bud cortex and the bud neck, yet Bni1p–1-596–GFP does so very weakly (Figure 1F). The difference between these two constructs is the region homologous to the DD. Because the DD region of mDia1 has been shown to facilitate dimerization (Li and Higgs, 2005), we asked whether dimerization might be important for localization. We tested whether artificially dimerizing the Bni1p–1-596 construct would allow it to localize appropriately. To do this, we appended a leucine zipper from human CREB, which functions as a dimerization domain (Schumacher *et al.*, 2000). The leucine zipper fused to GFP is cytoplasmic (Figure 1J), whereas the Bni1p–1-596–leucine-zipper construct localized robustly and broadly to the cell cortex and neck (Figure 1G). With this result in hand, we explored how much of the N-terminal domain, when dimerized, is necessary for this localization. We found that Bni1p–1-333–GFP does not localize to the bud cortex, whereas Bni1–1-333– leucine-zipper localizes to both the bud cortex and the bud neck (Figure 1, H and I). In addition, when the Bni1p–1-596 construct, which does not localize, is fused to a region (717–834) downstream of the DD domain, localization is restored (construct ΔDD 1-834, Figure 1K). Therefore the 717–834 region, which is predicted to form a coiled coil, might also contribute to the dimerization of the N-terminus of Bni1p.

The N-terminal half of Bni1p contains three localization regions

Our results define two regions of Bni1p that localize independently, namely residues 1–333 and 822–992. We next sought to determine whether the region between these two also contributes to localization. To our surprise, Bni1p–334-821–GFP, which covers the DID, DD, and the following predicted coiled-coil (CC) region before the SBD domain, was also able to localize to the bud cortex and bud neck (Figure 1L), similar to Bni1p–1-1239–GFP.

All the localizations were unchanged in *BNI1* cells (Supplemental Figure S1A), indicating that localization does not require dimerization with endogenous Bni1p. Thus three distinct localization determinants must exist in the bud and later at the neck. Moreover, the localization of Bni1p–1-333–leucine-zipper, Bni1p–334-821, or Bni1-GFP to the bud cortex is independent of the actin cytoskeleton, as they were unchanged when the actin cytoskeleton was completely disassembled by treating cells for 10 min with 200 μM of the actin-depolymerizing drug latrunculin A (Figure 1, M–O).

Thus Bni1p is localized to the bud cortex by three localization regions, which we will refer to as LD1, LD2, and LD3. LD1 resides in the N-terminal 333 amino acids containing the GBD and requires dimerization. LD2 resides in the 334–821 amino acids covering the DID-DD-CC domains. LD3 resides in the region of the Spa2p-binding domain. As we will discuss, Bni1p has a fourth localization region, LD4, encompassing residues 1231–1953.

N-terminally truncated Bni1p has compromised Bni1p localization and actin structure

To explore how important the localization domains are for growth, we made a series of constructs deleting progressively larger internal regions from Bni1p residue 79 up to the FH1 domain (Figure 2A). These constructs were targeted to the chromosomal locus so that the proteins were expressed as the sole copy from the endogenous *BNI1* promoter. Cells with these constructs expressed the appropriately sized proteins and were all viable (Figure 2, B and D). Moreover, growth at 25°C was unaffected by simultaneous deletion of *BNR1* (Figure 2B), in support of our earlier finding that yeast are viable expressing just the FH1–FH2 fragment of Bni1p as their sole formin protein (Gao and Bretscher, 2009). For ease of description, we have grouped the internal deletion series into two classes: class I deletions do not noticeably affect cell growth, whereas class II deletions, represented by the two largest internal deletions, *bni1Δ79-988-3GFP* and *bni1Δ79-1230-3GFP*, grew less well in both *BNR1* and *bnr1Δ* backgrounds (Figure 2B). In fact, class II internal deletions in the *BNR1* background grew less well than *BNR1 bni1Δ* cells.

We next examined the actin cytoskeleton and the localization of the Bni1p-derived constructs C-terminally tagged with 3GFP (Figure 2C and Table 2). In wild-type cells during bud growth, actin cables extend along the surface of the bud and into the mother cell, whereas actin patches concentrate in the bud. Phalloidin staining of class I *BNI1* deletion mutants reveals a modest disruption of their actin cytoskeleton, which becomes more noticeable

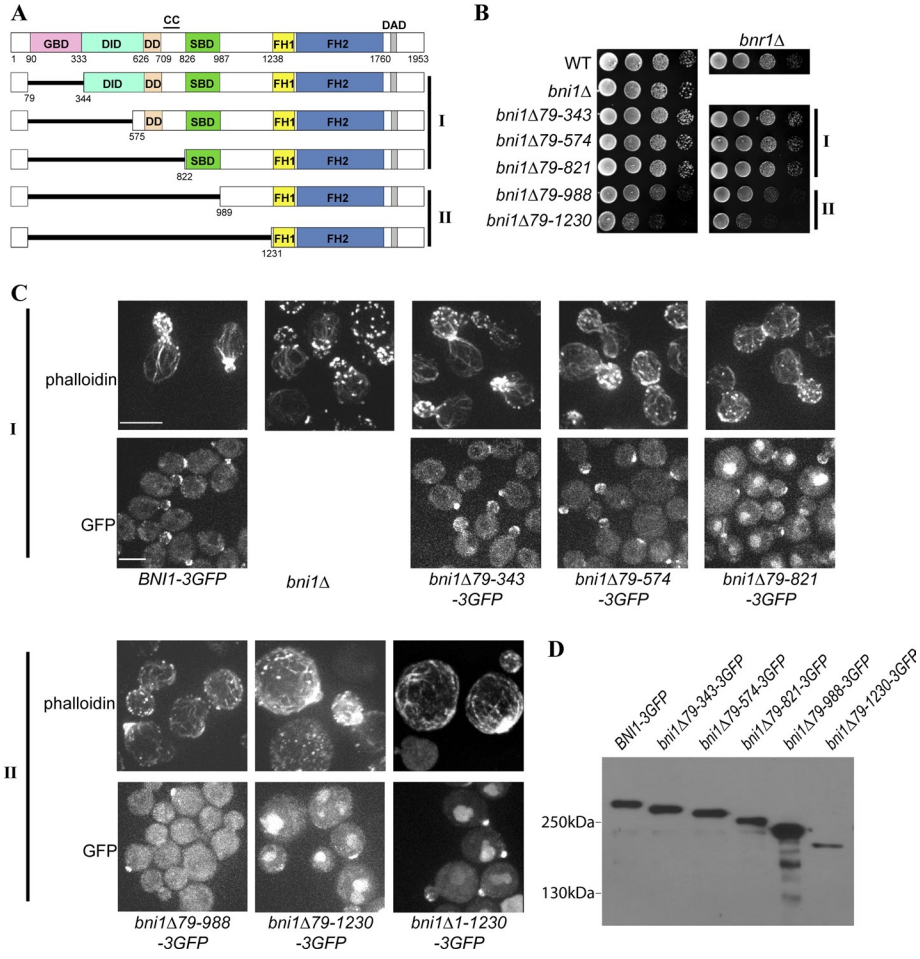

FIGURE 2: Deletion of N-terminal regions of Bni1p leads to progressive defects in growth and polarity. (A) Schematic diagram of *BNI1* truncation constructs, with the two phenotypic classes indicated. (B) Growth of 10-fold serial dilutions of cells with N-terminal deletions in a *BNR1* and *bnr1Δ* background grown at 26°C on yeast extract/peptone/dextrose (YPD) plates. (C) F-Actin staining with phalloidin and GFP localization of the indicated constructs in *BNR1* cells. Scale bars, 5 μm. (D) Immunoblot with antibodies against GFP to show expression of the indicated Bni1p constructs.

with increasing size of the internal deletion. In the class I construct with the largest deletion, *bni1-Δ79-821-3GFP*, the actin patches are somewhat polarized, and the actin cables are more disoriented and shorter, especially in the mother cells. Localization of the class I *BNI1* mutant proteins showed that in general they localized very similarly to wild-type Bni1p-3GFP, namely concentrating at the nascent bud site and the tips of small buds, in a crescent over the cortex of medium buds, and at the septal plane between dividing cells (Figure 2C). Despite this general similarity, *bni1Δ79-821-3GFP* localizes to the nucleus and less robustly to the cell cortex. However, in both class II *BNI1* mutants, actin cables are obviously short and disoriented, and actin patches are severely depolarized. This localization is independent of the first 78 amino acids, as *bni1Δ1-1230* shows the same localization (Figure 2C). The localization of the class II *BNI1* mutants was much weaker, being seen in a polarized manner only in unbudded and tiny budded cells. The localizations of these Bni1p mutants are summarized in Table 2.

Bni1p deletion constructs	Bud tip localization	Bud neck localization
Bni1p	+++	+++
Bni1Δ79-343p	+++	+++
Bni1Δ79-574p	+++	+++
Bni1Δ79-821p	++	+++
Bni1Δ79-988p	+	+
Bni1Δ79-1230p (LD4)	+	–
CRIB-Bni1Δ79-988p	+++	+++

Numbers indicate Bni1p amino acid residues present in the constructs. A plus or minus sign indicates whether the construct was detected by live imaging at the indicated place. The number of plus signs indicates how frequently it was seen in a log-phase culture.

TABLE 2: Localization of N-terminally truncated Bni1p constructs.

Because the constructs expressing just the FH1-FH2-COOH of Bni1p are localized at the beginning of the cell cycle, an additional localization determinant must exist in this region. This localization was also unchanged in cells treated with latrunculin A for 10 min (Supplemental Figure S2), showing that, in addition to the three N-terminal localization regions just documented, Bni1p has a fourth F-actin-independent localization region in the FH1-FH2-COOH part of Bni1p, namely LD4. No bud neck localization was observed for LD4, although note that these cells are depolarized and the morphological defect may affect neck recruitment (Figure 2C).

Spa2p has a function in addition to binding the SBD of Bni1p

The defining difference between the class I and class II internal deletions of Bni1p is the presence or absence of the SBD. If Spa2p is an important determinant for Bni1p localization, one would predict that combining *spa2Δ* with class I *BNI1* mutants should phenocopy a class II mutant. Indeed, combining class I mutants with *spa2Δ* compromised the growth of the cells in a progressive manner, with the larger deletions being more affected (Figure 3A). To explore the basis for these growth defects, the actin cytoskeleton and localization of the Bni1p-3GFP truncated proteins were examined. When *spa2Δ* was combined with the class I mutants, actin structures were more disrupted, especially in *bni1Δ79-821 spa2Δ* cells, which had greatly reduced cables and depolarized actin patches. The localization of the Bni1p-deletion constructs was also affected, with the larger deletions being the most severe (Figure 3B).

We next examined the effect of combining *spa2Δ* with the class II *BNI1* deletion mutants, which lack the SBD, and found, unexpectedly, that they show synthetic lethality (Figure 3C). Thus, although the SBD is not present in these Bni1p constructs, Spa2p is essential for the viability of these cells, indicating that Spa2p has an important function independent of its interaction with the SBD of Bni1p.

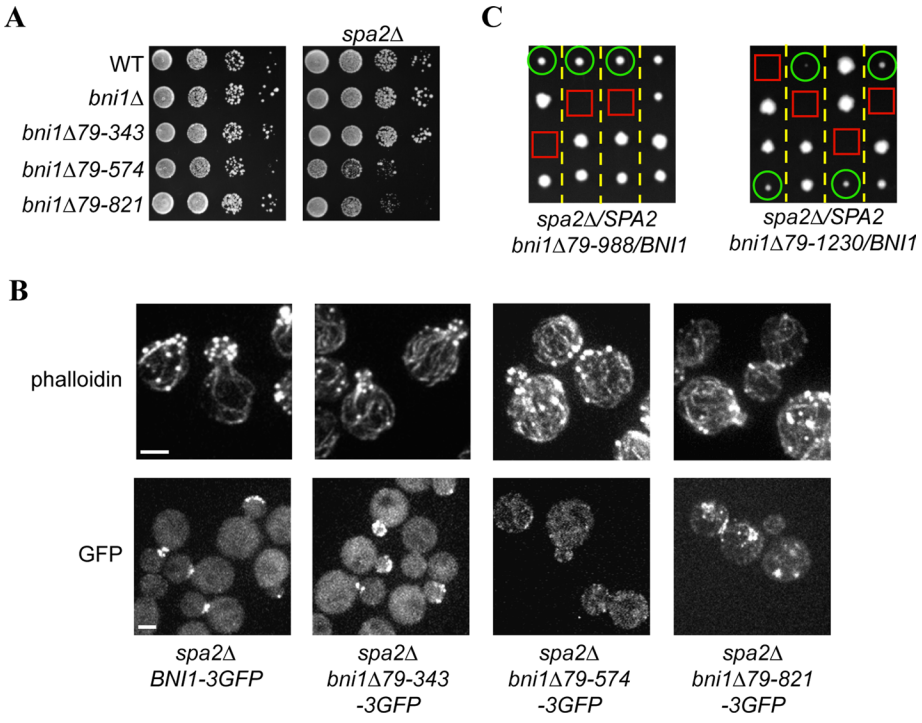

FIGURE 3: Spa2p contributes to cell growth both through binding the SBD of Bni1p and independent of the SBD. (A) Growth assays of class I Bni1p truncations in *SPA2* and *spa2*Δ cells at 26°C on YPD plates. (B) F-Actin staining with phalloidin and GFP localization of the indicated constructs in *spa2*Δ cells. Scale bar, 2 μm. (C) Growth of spores derived from individual tetrads (arrayed vertically) after sporulation of the indicated diploids. Circles indicate *bni1*Δ*79-988* or *bni1*Δ*79-1230 SPA2* spores; rectangles indicate *bni1*Δ*79-988* or *bni1*Δ*79-1230 spa2*Δ spores.

The N-terminal region of Bni1p is required for spindle orientation

We recently reported that yeast is viable when the only formin present is a construct of just the FH1 plus FH2 domains of either Bni1p or Bnr1p (Gao and Bretscher, 2009). This implies that the N-terminal localization regions described earlier are not essential for cell growth. To study the role of N-terminal localization regions in Bni1p's function, we sought a more stringent condition for cell growth. It has been reported that spindle orientation, necessary for proper nuclear segregation, requires either the Kar9p/Myo2p/Bni1p pathway or the dynein/dynactin pathway, with either being dispensable for spindle orientation, but defects in both being lethal (Fujiwara *et al.*, 1999; Miller *et al.*, 1999; Tong *et al.*, 2001). The Kar9p/Myo2p/Bni1p pathway has been shown to involve the binding of Myo2p to Kar9p on the ends of cytoplasmic microtubules for transport along Bni1p-nucleated actin cables into the bud (Yeh *et al.*, 2000; Yin *et al.*, 2000; Hwang *et al.*, 2003). Because Arp1p is a core component of the dynactin complex, disruption of *ARP1* leads to the disassembly of the dynactin complex (Schroer, 2004). Thus in *arp1*Δ cells, actin cables nucleated and oriented by localized Bni1p should be essential for spindle orientation and thereby provide a genetic system to study the role of the localization regions of Bni1p in its function.

When we combined *bni1*Δ with *arp1*Δ we were surprised to find that a *bni1*Δ *arp1*Δ (and a *bni1*Δ *dyn1*Δ; Supplemental Figure S3A) strain is viable, thereby in principle compromising the design of our study and supporting alternative observations of others (Lee *et al.*, 1999; Yeh *et al.*, 2000). Fortuitously, when we combined *arp1*Δ with the class I and class II series of internal deletions in Bni1p we uncovered a clear finding: class I deletions are viable in conjunction with *arp1*Δ, whereas class II deletions are inviable in conjunction with *arp1*Δ (Figure 4A).

To explore the potential role of the Bni1p localization determinants in spindle orientation, we examined the class I mutants in more detail in both *ARP1* and *arp1*Δ cells. Because these processes require microtubules that are less stable at low temperature, we examined the sensitivity of the strains for growth at 14°C and in the presence of sublethal levels of the microtubule-destabilizing drug benomyl (Figure 4B). In *ARP1* cells, class I mutants like *bni1*Δ showed no cold or benomyl sensitivity (Figure 4B). However, in the *arp1*Δ background, the largest internal deletion of class I mutants, *bni1*Δ*79-821*, shows more cold and benomyl sensitivity than *bni1*Δ *arp1*Δ cells (Figure 4B), suggesting that class I truncations are at least somewhat compromised in microtubule-mediated spindle orientation. Consistent with this phenotype, DNA staining of class I truncations in *ARP1* cells revealed that they have a modest defect in nuclear segregation at 16°C, similar to a *bni1*Δ cell, and this defect is strongly exacerbated in *arp1*Δ cells (Figure 4C). The binuclear phenotype, as well as cold and benomyl sensitivity, suggests that *BNI1* class I mutants have defects in spindle orientation. Indeed, the spindle orientation in small- to medium-budded cells was observed using GFP-Tub1p and confirmed that Bni1p class I mutants exacerbate the spindle orientation defects seen in *arp1*Δ cells (Figure 4D).

Class II mutants in *ARP1* cells are cold sensitive and benomyl sensitive by themselves, displaying more severe microtubule-related defects than *bni1*Δ cells (Figure 4E), indicating that they have a negative gain of function in spindle orientation. Consistent with this interpretation, heterozygous *BNI1*/class II mutants in *arp1*Δ/*arp1*Δ cells also exhibited greater cold and benomyl sensitivity than *BNI1*/*bni1*Δ *arp1*Δ/*arp1*Δ cells (Figure 4F).

Inappropriate actin assembly is responsible for the phenotype of class II mutants

Because the essential role of Bni1p in *S. cerevisiae* is to nucleate and assemble actin cables, we asked whether the dominant phenotypes caused by the class II Bni1p mutants are related to their ability to assemble actin filaments at inappropriate locations. We first tested this model by mutating the FH2 domain of a class II truncation by changing a single amino acid (I1431A) that has been reported to abolish actin assembly activity (Xu *et al.*, 2004). Expression of *bni1*Δ*79-988* with the I1431A mutation is not synthetically lethal with *arp1*Δ and is not cold sensitive, behaving similarly to a *bni1*Δ mutation (Figure 5, A and B). Thus the deleterious phenotypes caused by *bni1*Δ*79-988* are due to its actin assembly activity.

Because the class II construct Bni1Δ79-988p–3GFP is poorly localized (Figure 2C), we explored whether the growth defects are due to mislocalized actin assembly. To test this, we fused the Cdc42-Rac interactive binding (CRIB) domain of Gic2p to the N-terminus of this class II mutant. Gic2p is a Cdc42p effector that is localized to the bud tip during bud growth and bud neck during cytokinesis by binding through its CRIB domain to Cdc42-GTP

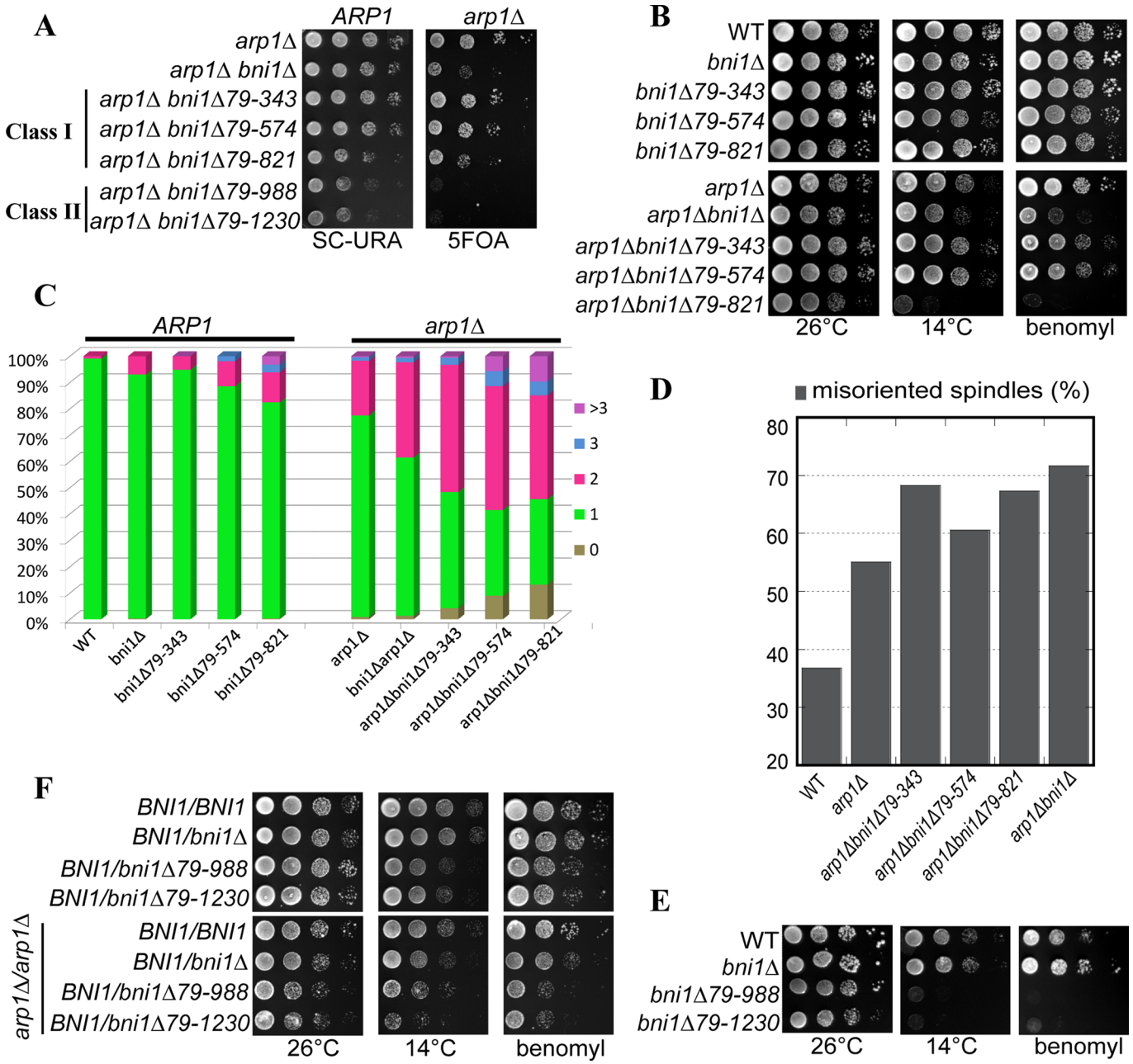

FIGURE 4: Deletion of N-terminal regions of Bni1p leads to progressive defects in nuclear segregation. (A) Growth of 10-fold serial dilutions of cells with N-terminal deletions in *ARP1* (SC-URA plates that retain the *CEN-URA3-ARP1* plasmid) and *arp1*Δ (5-fluoroorotic acid plates that select against the *CEN-URA3-ARP1* plasmid) cells grown at 26°C. (B) Growth of 10-fold serial dilutions of cells with class I N-terminal deletions in *ARP1* and *arp1*Δ cells at either at 26 or 14°C on YPD plates or at 26°C in the presence of 10 μg/ml benomyl. (C) Percentage of class I deletions in *ARP1* and *arp1*Δ cells with the indicated number of nuclei in the mother cell. Cells were grown at room temperature until OD = 0.2 and then shifted to 16°C for 8 h, and >500 cells were analyzed following staining with 4′,6-diamidino-2-phenylindole. (D) Percentage of cells with misoriented spindles in small- to medium-budded cells. n > 100 for each sample. (E, F) Growth of 10-fold serial dilutions of cells as indicated under the same conditions used in B.

(Burbelo *et al.*, 1995; Brown *et al.*, 1997). The addition of the CRIB domain to Bni1pΔ79-988 largely restored its localization to the bud cortex and also rescued the cold sensitivity (Figure 5, C and D). In addition, phalloidin staining showed polarized actin patches and directed actin cables in *CRIB-bni1Δ79-988* cells (Figure 5D). Therefore the deleterious phenotypes associated with class II mutants are a result of their ability to assemble mislocalized actin filaments.

DISCUSSION

To perform their physiological functions in actin assembly, formins need to be appropriately localized. Despite this critical aspect, remarkably little is known about how they are localized. It is clear for the mDia proteins that the N-terminal region is important for localization (Seth *et al.*, 2006; Brandt *et al.*, 2007; Gorelik *et al.*, 2011). In the recent study of Gorelik *et al.* (2011), a basic domain N-terminal to GBD was found to be important for plasma membrane localization,

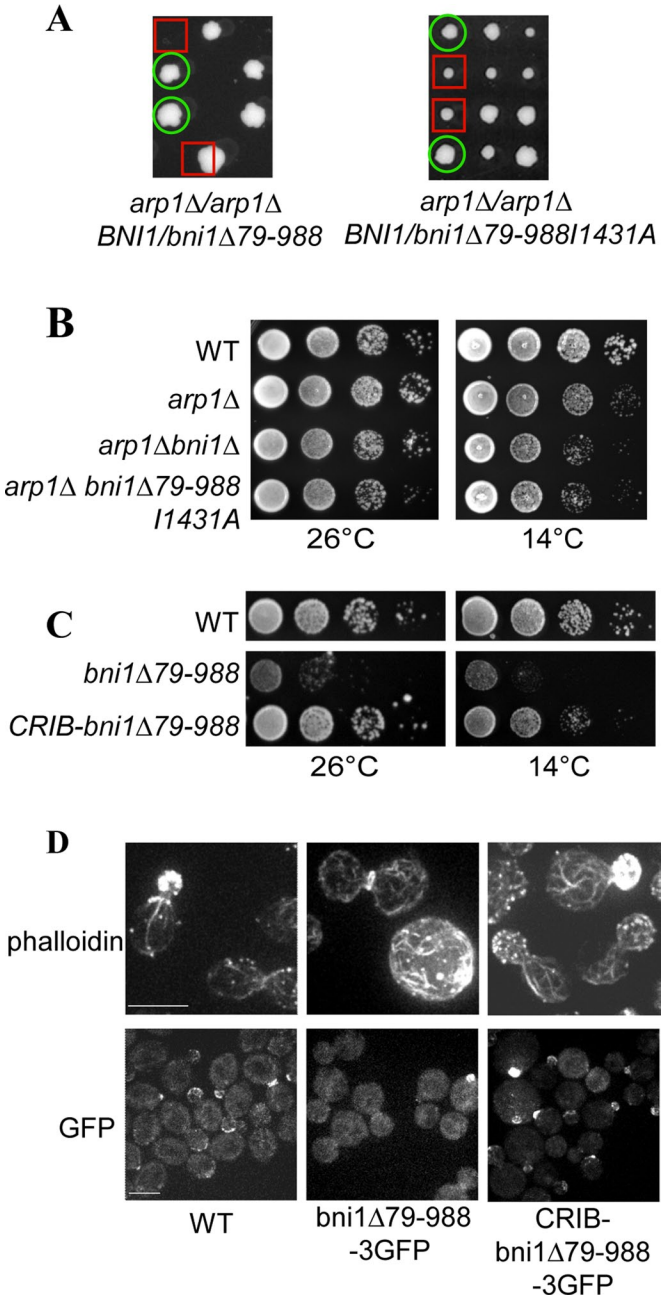

FIGURE 5: The dominant effects of a class II Bni1p deletion are due to mislocalized assembly of actin. (A) Growth of spores derived from individual tetrads (arrayed vertically) after sporulation of the indicated diploids. Circles indicate *BNI1 arp1*Δ spores; rectangles indicate *bni1*Δ*79-998 arp1*Δ or *bni1*Δ*79-998-I1431A arp1*Δ spores. (B) Growth of 10-fold serial dilutions of cells with the indicated genotypes on YPD plates at 26 and 14°C. (C) Growth of cells expressing *bni1*Δ*79-988* without or with an appended N-terminal CRIB domain. (D) F-Actin staining with phalloidin and GFP localization of the indicated construct. Scale bars, 5 μm.

and the small GTPase Rif could also contribute significantly, implying that these two factors work together for correct localization.

We took this type of analysis one step further in our identification of regions in Bni1p involved in its localization and sought to understand the functions of the identified localization domains. This analysis showed an unexpected complexity by revealing that Bni1p has at least four independent localization domains that can target the protein to the cell cortex in a manner independent of either endogenous Bni1p or filamentous actin. Three of these localization domains reside in the N-terminal 1200 residues of the protein and are independent of an actin cytoskeleton. LD1 (residues 1–333) coincides well with a region homologous to the structurally defined GBD domain. Formins of the Diaphanous family are regulated by binding to active Rho proteins, and this binding occurs through both the GBD region and the DID (Rose *et al.*, 2005). The need for dimerization probably reflects a low affinity of the isolated domain for the cell cortex, so that only with the higher affinity of a dimer is the interaction clear. Native Bni1p is presumably a dimer, as the DD domain, as well as the FH2 domain, can dimerize (Moseley *et al.*, 2004; Xu *et al.*, 2004; Otomo *et al.*, 2005). The second localization domain, LD2 (residues 334–834), includes the DID, the DD, and a region predicted to form a coiled coil. By virtue of the DD and predicted coiled-coil domain, this region almost certainly dimerizes. This region seems to be the most robust localization region, as the internal deletion constructs retaining it localize well in both *SPA2* and *spa2*Δ cells, whereas those lacking it localize poorly, especially in *spa2*Δ cells. Finally, LD3 encompassing the SBD has been identified as being important for Bni1p localization (Fujiwara *et al.*, 1998; Ozaki-Kuroda *et al.*, 2001). We identified all of these localization domains in cells in which the constructs were overexpressed. The fact that they localized suggests that the factors that localize them to the bud cortex or bud tip are likely to be much more abundant than endogenous Bni1p. In support of this conclusion, attempts to disrupt the function of endogenous Bni1p by expression of N-terminal constructs failed to cause any obvious phenotype. In addition to the three N-terminal localization domains, we found that the complementary C-terminal part LD4 (1231–1963), comprising the FH1, FH2, and C-terminal region, also has a weak localization domain to incipient and small buds. This localization is independent of either endogenous Bni1p or the presence of filamentous actin.

Having identified four localization domains in Bni1p, we sought to investigate their functions. Our original strategy assumed that correct localization is an essential part of formin function, so a deletion analysis of Bni1p regions in a *bnr1*Δ cell should reveal the essential localization domain. Accordingly, we made a series of N-terminal deletions in the chromosomal copy of Bni1p and assessed their effect on growth in *BNR1* and *bnr1*Δ cells. During this analysis, we made the unexpected discovery that yeast can grow remarkably well in the absence of a localized formin, namely when the only formin protein present was the delocalized FH1 plus FH2 domain of either Bni1p or Bnr1p (Gao and Bretscher, 2009). Despite this result, the N-terminal deletions of Bni1p were very informative. Deleting up to the SBD had little effect on growth, whereas deleting more of the N-terminal region to remove the SBD was deleterious to growth and resulted in quite depolarized cells that, even in the presence of Bnr1p, conferred a more severe phenotype than *bni1*Δ. Expression of this region of Bni1p therefore confers a dominant-negative phenotype.

Before this study, the only identified localization mechanisms for Bni1p were provided by Spa2p through the SBD (Fujiwara *et al.*, 1998; Ozaki-Kuroda *et al.*, 2001) and potentially through the polarisome-associated Bud6p to the C-terminal region (Ozaki-Kuroda *et al.*, 2001). Because N-terminal deletion constructs containing the SBD were relatively healthy, whereas those lacking it were dominant negative, we suspected that combining *spa2*Δ with our Bni1p constructs containing the SBD should phenocopy those lacking it. *spa2*Δ indeed compromised growth of Bni1p constructs with the SBD. It is surprising that the dominant-negative Bni1p constructs

Strain	Genotype	Source
ABY1848	MATa/α *his3Δ1/ his3Δ1 leu2Δ0/ leu2Δ0 ura3Δ0/ ura3Δ0 met15Δ0/MET15 lys2Δ0/LYS2*	Evangelista *et al.* (2002)
ABY1801	MAT a/α *his3Δ1/ his3Δ1 leu2Δ0/ leu2Δ0 met15?/met15? lys2?/lys2? ura3Δ0/ ura3Δ0 bnr1Δ::KanR/ bnr1Δ::KanR*	Gao *et al.* (2010)
ABY2838	MATa/α *his3Δ1/ his3Δ1 leu2Δ0/ leu2Δ0 ura3Δ0/ ura3Δ0 met15Δ0/met15Δ0 bni1Δ::KanR/ bni1Δ::KanR*	This study
ABY3280	MATa *his3Δ1 leu2Δ0 ura3Δ0 met15Δ0 spa2Δ::Kan^R*	Invitrogen
ABY2856	MATa *his3Δ1 leu2Δ0 ura3Δ0 met15Δ0 bni1Δ79-343::LEU2*	This study
ABY2857	MATa *his3Δ1 leu2Δ0 ura3Δ0 met15Δ0 bni1Δ79-574::LEU2*	This study
ABY2858	MATa *his3Δ1 leu2Δ0 ura3Δ0 met15Δ0 bni1Δ79-821::LEU2*	This study
ABY2859	MATa *his3Δ1 leu2Δ0 ura3Δ0 met15Δ0 bni1Δ79-988::LEU2*	This study
ABY2854	MATa *his3Δ1 leu2Δ0 ura3Δ0 met15Δ0 bni1Δ79-1230::LEU2*	This study
ABY2887	MATa *his3Δ1 leu2Δ0 ura3Δ0 met15? lys2? bnr1Δ::Kan^R bni1Δ79-343::LEU2*	This study
ABY2888	MATa *his3Δ1 leu2Δ0 ura3Δ0 met15? lys2? bnr1Δ::Kan^R bni1Δ79-574::LEU2*	This study
ABY2889	MATa *his3Δ1 leu2Δ0 ura3Δ0 met15? lys2? bnr1Δ::Kan^R bni1Δ79-821::LEU2*	This study
ABY2890	MATa *his3Δ1 leu2Δ0 ura3Δ0 met15? lys2? bnr1Δ::Kan^R bni1Δ79-988::LEU2*	This study
ABY2891	MATa *his3Δ1 leu2Δ0 ura3Δ0 met15? lys2? bnr1Δ::Kan^R bni1Δ79-1230::LEU2*	This study
ABY3090	MATa/α *his3Δ1/ his3Δ1 leu2Δ0/ leu2Δ0 ura3Δ0/ ura3Δ0 met15Δ0/MET15 lys2Δ0/LYS2 BNI1/ BNI1-3GFP*	This study
ABY3092	MAT a/α *his3Δ1/ his3Δ1 leu2Δ0/ leu2Δ0 met15?/met15? lys2?/lys2? ura3Δ0/ ura3Δ0 bni1Δ79-343::LEU2/ bni1Δ79-343-3GFP::LEU2, URA3*	This study
ABY3093	MAT a/α *his3Δ1/ his3Δ1 leu2Δ0/ leu2Δ0 met15?/met15? lys2?/lys2? ura3Δ0/ ura3Δ0 bni1Δ79-574::LEU2/ bni1Δ79-574-3GFP::LEU2, URA3*	This study
ABY3094	MAT a/α *his3Δ1/ his3Δ1 leu2Δ0/ leu2Δ0 met15?/met15? lys2?/lys2? ura3Δ0/ ura3Δ0 bni1Δ79-821::LEU2/ bni1Δ79-821-3GFP::LEU2, URA3*	This study
ABY3095	MAT a/α *his3Δ1/ his3Δ1 leu2Δ0/ leu2Δ0 met15?/met15? lys2?/lys2? ura3Δ0/ ura3Δ0 bni1Δ79-988::LEU2/ bni1Δ79-988-3GFP::LEU2, URA3*	This study
ABY3096	MAT a/α *his3Δ1/ his3Δ1 leu2Δ0/ leu2Δ0 met15?/met15? lys2?/lys2? ura3Δ0/ ura3Δ0 bni1Δ79-1230::LEU2/ bni1Δ79-1230-3GFP::LEU2, URA3*	This study
ABY3283	MATa *his3Δ1 leu2Δ0 ura3Δ0 met15? lys2? spa2Δ::KanR bni1Δ79-343-3GFP::LEU2,URA3*	This study
ABY3284	MATa *his3Δ1 leu2Δ0 ura3Δ0 met15? lys2? spa2Δ::KanR bni1Δ79-574-3GFP::LEU2,URA3*	This study
ABY3285	MATa *his3Δ1 leu2Δ0 ura3Δ0 met15? lys2? spa2Δ::KanR bni1Δ79-821-3GFP::LEU2,URA3*	This study
ABY2851	MATa/α *his3Δ1/ his3Δ1 leu2Δ0/ leu2Δ0 ura3Δ0/ ura3Δ0 met15Δ0/met15Δ0 arp1Δ::Kan^R/ arp1Δ::Kan^R BNI1/ bni1Δ79-988::LEU2*	This study
ABY2852	MATa/α *his3Δ1/ his3Δ1 leu2Δ0/ leu2Δ0 ura3Δ0/ ura3Δ0 met15Δ0/met15Δ0 arp1Δ::Kan^R/ arp1Δ::Kan^R BNI1/ bni1Δ79-1230::LEU2*	This study
ABY2860	MAT? *his3Δ1 leu2Δ0 ura3Δ0 met15Δ0 arp1Δ::Kan^R bni1Δ79-343::LEU2*	This study
ABY2861	MAT? *his3Δ1 leu2Δ0 ura3Δ0 met15Δ0 arp1Δ::Kan^R bni1Δ79-574::LEU2*	This study
ABY2862	MAT? *his3Δ1 leu2Δ0 ura3Δ0 met15Δ0 arp1Δ::Kan^R bni1Δ79-821::LEU2*	This study
ABY2881	MATa/α *his3Δ1/ his3Δ1 leu2Δ0/ leu2Δ0 ura3Δ0/ ura3Δ0 met15Δ0/met15Δ0 arp1Δ::Kan^R/ arp1Δ::Kan^R BNI1/ bni1Δ79-988 I1431A::LEU2*	This study
ABY3007	MATa/α *his3Δ1/ his3Δ1 leu2Δ0/ leu2Δ0 ura3Δ0/ ura3Δ0 met15Δ0/met15Δ0 CRIB-bni1Δ79-988::LEU2/CRIB-bni1Δ79-988::LEU2*	This study
ABY2897	MATa/α *his3Δ1/ his3Δ1 leu2Δ0/ leu2Δ0 ura3Δ0/ ura3Δ0 met15Δ0/met15Δ0 bni1Δ79-988::LEU2/ bni1Δ79-988::LEU2*	This study

TABLE 3: Yeast strains used in this study.

that lack the SBD are synthetically lethal with *spa2Δ*, indicating that Spa2p performs a function in addition to binding the SBD of Bni1p. One possibility is that Spa2p is still contributing to Bni1p localization through Bud6p, which binds both Spa2p and the C-terminal region of Bni1p (Evangelista *et al.*, 1997; Sheu *et al.*, 1998; Moseley and Goode, 2005).

Because Bni1p localization is not essential for viability in *bnr1*Δ cells, we explored the possibility of exploiting a situation in which Bni1p localization is important even in the presence of Bnr1p. Spindle orientation is required for proper nuclear segregation and depends both on the Bni1p/Myo2p/Kar9p pathway and the dynactin/dynein pathway. In the absence of the dynein/dynactin pathway, Bni1p/Myo2p/Kar9p becomes the critical mechanism for spindle orientation. We therefore combined our N-terminal Bni1p deletion series with *arp1*Δ cells, lacking a component of the dynactin complex. Indeed, we found a modest spindle orientation defect (as determined by benomyl sensitivity and the fraction of mother cells with two or more nuclei) in the mutants even in *ARP1* cells that increased as additional localization domains were deleted from the N-terminal region of Bni1p, and these defects were strongly enhanced in *arp1*Δ cells. Therefore all the identified N-terminal localization domains contribute to the Bni1p-dependent spindle orientation pathway. As described earlier, Bni1p constructs from which all the N-terminal localization domains were deleted had a dominant-negative effect on growth and were found to be inviable with *arp1*Δ. The dominant-negative effects could be abrogated by either mutating the Bni1p construct to eliminate its actin-nucleating ability or adding the Cdc42-binding CRIB domain from Gic2p to enhance its localization to growth sites. Therefore the dominant-negative effects are due to inappropriate localization of actin assembly that affects both polarized growth and spindle orientation.

The results presented in this study reveal that Bni1p has four localization domains and they contribute cumulatively to Bni1p's function in polarized growth and spindle orientation. It is surprising that so many independent localization domains exist in one protein. However, multiple N-terminal localization domains seem to be a common property of yeast formin proteins, as Bnr1p has two separate localization domains, encompassing residues 1–466, and 466–733 (Gao *et al.*, 2010). These findings could suggest that the cell needs very careful and intimate control of Bni1p to coordinate its localization, and hence cable assembly, with all the other events going on at sites of growth. The strict regulation of formin proteins could be common for higher organisms, as they often possess multiple formin isoforms (Higgs, 2005). Alternatively, the many localization domains may be used under other growth conditions, for example, during shmooing, or during the highly polarized growth that occurs during filamentous growth. The finding of four distinct localization domains implies that four different mechanisms may be involved in localizing Bni1p. Identifying these mechanisms is the next critical step in this analysis.

MATERIALS AND METHODS

Yeast strains and molecular biology techniques

The strains used in this study are listed in Table 3. All strains were generated in the S288C strain background derived from the deletion consortium (Brachmann *et al.*, 1998). Standard media and techniques for growing and transforming yeast were used (Sherman, 1991). The plasmids used in this study are listed in Table 4. Bni1p N-terminal overexpression plasmids were made using the pRS316 *GAL1-10* vector pHL012 (Liu *et al.*, 1992) and different Bni1p regions inserted into the *Bam*HI and *Mlu*I restriction sites. GFP was appended using the *Mlu*I and *Not*I sites. To express the different Bni1p constructs, the relevant strains were first grown overnight in 5 ml SC-URA media containing 2% raffinose to an OD_{600} of 0.4, and then 0.5 ml of 20% galactose was added to the media and growth continued for 3–4 h. Growth assays were performed using 1:10 dilutions.

Plasmid	Backbone	Genotype
pHL012	pRS316	$P_{GAL1-10}$
pWL062	pRS316	$P_{GAL1-10}$-*BNI1 (1-1953)-GFP*
pWL150	pRS316	$P_{GAL1-10}$-*BNI1 (1-333)-GFP*
pWL151	pRS316	$P_{GAL1-10}$-*BNI1 (1-333)-leucine zipper-GFP*
pWL054	pRS316	$P_{GAL1-10}$-*BNI1 (1-596)-GFP*
pWL071	pRS316	$P_{GAL1-10}$-*BNI1 (1-596)-leucine zipper-GFP*
pWL060	pRS316	$P_{GAL1-10}$-*BNI1 (1-717)-GFP*
pWL055	pRS316	$P_{GAL1-10}$-*BNI1 (1-834)-GFP*
pWL148	pRS316	$P_{GAL1-10}$-*BNI1 (334-834)-GFP*
pWL099	pRS316	$P_{GAL1-10}$-*BNI1 (1-834Δ596-717)-GFP*
pWL067	pRS316	$P_{GAL1-10}$-*BNI1 (1-1239)-GFP*
pWL117	pRS316	$P_{GAL1-10}$-*BNI1 (501-717)-GFP*
pWL084	pRS316	$P_{GAL1-10}$-*GFP-BNI1 (822-992)-GFP*
pWL108	pRS316	$P_{GAL1-10}$-*BNI1 (592-834)-GFP*
pWL107	pRS316	$P_{GAL1-10}$-*BNI1 (987-1239)-GFP*
pWL031	pRS305	P_{BNI1}-*BNI1 (1-79)-BNI1 (344-1953)*
pWL032	pRS305	P_{BNI1}-*BNI1 (1-79)-BNI1 (575-1953)*
pWL033	pRS305	P_{BNI1}-*BNI1 (1-79)-BNI1 (822-1953)*
pWL034	pRS305	P_{BNI1}-*BNI1 (1-79)-BNI1 (989-1953)*
pWL027	pRS305	P_{BNI1}-*BNI1 (1-79)-BNI1 (1231-1953)*
pWL085	pRS306	*BNI1C-3GFP-BNI13′*
pWL042	pRS316	P_{ARP1}-*ARP1(1-1155)*
pWL046	pRS305	P_{BNI1}-*BNI1 (1-79)-BNI1 (989-1953 I1431A)*
pWL069	pRS305	P_{BNI1}-*BNI1 (1-79)-CRIB-BNI1 (989-1953)*
CUB1210	pRS403	P_{TUB1}-*GFP-TUB1*

TABLE 4: Plasmids used in this study.

To make Bni1 internal deletion integration plasmids, 481 base pairs of the Bni1p promoter region with the first 79 amino acids of *BNI1* (flanked by *Bam*HI and *Mlu*I) were ligated with different C-terminal regions of *BNI1* (flanked by *Mlu*I and *Not*I) and then ligated with −693 to −480 base pairs of the *BNI1* promoter region (flanked by *Not*I and *Pac*I) into the vector pRS305. The Bni1p internal deletion integration plasmids were then cut with *Not*I and transformed into appropriate strains to get the integrated *BNI1* internal deletions.

To tag genomic *BNI1* or *BNI1* deletions with 3GFP, plasmid pWL085 was constructed using integration vector pRS306. Four DNA fragments were ligated together: *BNI1 3′ UTR* 6021–6171 base pairs (flanked by *Kpn*I and *Sal*I), the C-terminal coding region of *BNI1* 5500–5859 base pairs (flanked by *Sal*I and *Bam*HI), DNA encoding *3GFP* (flanked by *Bam*HI and *Not*I), and *BNI1 3′ UTR* 5863–6020 base pairs (flanked by *Not*I and *Sac*I). This *Kpn*1–*Sac*1 fragment was then ligated into a similarly cut pRS306 vector to give pWL085. pWL085 was then digested with *Sal*I for integration at the C-terminus of *BNI1*.

Microscopy

For live-cell imaging, cells were placed under 2% agarose in synthetic medium, with appropriate amino acids. Images were acquired on a spinning disk confocal system (3I Corp, Denver, CO) using a DMI 6000B microscope (Leica, Wetzlar, Germany) and a digital camera (QuantEM; Photometrics, Tucson, AZ). Images were then further analyzed and adjusted using SlideBook 5 (Intelligent Imaging Innovations, Denver, CO). To disrupt actin structures, cells were treated with 200 μM latrunculin A for 10 min. The actin cytoskeleton was visualized after formaldehyde fixation and staining with Alexa 568–phalloidin.

Spindle orientation

To visualize spindles, plasmid CUB1210 was linearized with *Xba*I and integrated into the *TUB1* locus. Cells were grown at room temperature until mid-log phase, and spindle orientation was scored using GFP-Tub1p in small- to medium-budded cells. At least 100 cells were analyzed for each data point as described (Yin *et al.*, 2000).

Protein extracts and immunoblotting

Protein extraction and immunoblotting with mouse anti-GFP monoclonal antibody (Santa Cruz Biotechnology) at 1:200 was performed as described (Santiago-Tirado *et al.*, 2011).

ACKNOWLEDGMENTS

We are very grateful to members of the Bretscher lab for comments on the manuscript. We also thank Tim Huffaker for providing plasmids that made this study possible. This work was supported by National Institutes of Health Grant GM39066.

REFERENCES

Beach DL, Thibodeaux J, Maddox P, Yeh E, Bloom K (2000). The role of the proteins Kar9 and Myo2 in orienting the mitotic spindle of budding yeast. Curr Biol 10, 1497–1506.

Brachmann CB, Davies A, Cost GJ, Caputo E, Li J, Hieter P, Boeke JD (1998). Designer deletion strains derived from *Saccharomyces cerevisiae* S288C: a useful set of strains and plasmids for PCR-mediated gene disruption and other applications. Yeast 14, 115–132.

Brandt DT, Marion S, Griffiths G, Watanabe T, Kaibuchi K, Grosse R (2007). Dia1 and IQGAP1 interact in cell migration and phagocytic cup formation. J Cell Biol 178, 193–200.

Brown JL, Jaquenoud M, Gulli MP, Chant J, Peter M (1997). Novel Cdc42-binding proteins Gic1 and Gic2 control cell polarity in yeast. Genes Dev 11, 2972–2982.

Burbelo PD, Drechsel D, Hall A (1995). A conserved binding motif defines numerous candidate target proteins for both Cdc42 and Rac GTPases. J Biol Chem 270, 29071–29074.

Buttery SM, Yoshida S, Pellman D (2007). Yeast formins Bni1 and Bnr1 utilize different modes of cortical interaction during the assembly of actin cables. Mol Biol Cell 18, 1826–1838.

Chesarone MA, DuPage AG, Goode BL (2010). Unleashing formins to remodel the actin and microtubule cytoskeletons. Nat Rev Mol Cell Biol 11, 62–74.

Delgehyr N, Lopes CS, Moir CA, Huisman SM, Segal M (2008). Dissecting the involvement of formins in Bud6p-mediated cortical capture of microtubules in *S. cerevisiae*. J Cell Sci 121, 3803–3814.

Evangelista M, Blundell K, Longtine MS, Chow CJ, Adames N, Pringle JR, Peter M, Boone C (1997). Bni1p, a yeast formin linking cdc42p and the actin cytoskeleton during polarized morphogenesis. Science 276, 118–122.

Evangelista M, Pruyne D, Amberg DC, Boone C, Bretscher A (2002). Formins direct Arp2/3-independent actin filament assembly to polarize cell growth in yeast. Nat Cell Biol 4, 260–269.

Fujiwara T, Tanaka K, Inoue E, Kikyo M, Takai Y (1999). Bni1p regulates microtubule-dependent nuclear migration through the actin cytoskeleton in *Saccharomyces cerevisiae*. Mol Cell Biol 19, 8016–8027.

Fujiwara T, Tanaka K, Mino A, Kikyo M, Takahashi K, Shimizu K, Takai Y (1998). Rho1p-Bni1p-Spa2p interactions: implication in localization of Bni1p at the bud site and regulation of the actin cytoskeleton in *Saccharomyces cerevisiae*. Mol Biol Cell 9, 1221–1233.

Gao L, Bretscher A (2009). Polarized growth in budding yeast in the absence of a localized formin. Mol Biol Cell 20, 2540–2548.

Gao L, Liu W, Bretscher A (2010). The yeast formin Bnr1p has two localization regions that show spatially and temporally distinct association with septin structures. Mol Biol Cell 21, 1253–1262.

Gorelik R, Yang C, Kameswaran V, Dominguez R, Svitkina T (2011). Mechanisms of plasma membrane targeting of formin mDia2 through its amino terminal domains. Mol Biol Cell 22, 189–201.

Higgs HN (2005). Formin proteins: a domain-based approach. Trends Biochem Sci 30, 342–353.

Hwang E, Kusch J, Barral Y, Huffaker TC (2003). Spindle orientation in *Saccharomyces cerevisiae* depends on the transport of microtubule ends along polarized actin cables. J Cell Biol 161, 483–488.

Lammers M, Rose R, Scrima A, Wittinghofer A (2005). The regulation of mDia1 by autoinhibition and its release by Rho*GTP. EMBO J 24, 4176–4187.

Lee L, Klee SK, Evangelista M, Boone C, Pellman D (1999). Control of mitotic spindle position by the *Saccharomyces cerevisiae* formin Bni1p. J Cell Biol 144, 947–961.

Li F, Higgs HN (2003). The mouse formin mDia1 is a potent actin nucleation factor regulated by autoinhibition. Curr Biol 13, 1335–1340.

Li F, Higgs HN (2005). Dissecting requirements for auto-inhibition of actin nucleation by the formin, mDia1. J Biol Chem 280, 6986–6992.

Li YY, Yeh E, Hays T, Bloom K (1993). Disruption of mitotic spindle orientation in a yeast dynein mutant. Proc Natl Acad Sci USA 90, 10096–10100.

Liu H, Krizek J, Bretscher A (1992). Construction of a GAL1-regulated yeast cDNA expression library and its application to the identification of genes whose overexpression causes lethality in yeast. Genetics 132, 665–673.

Miller RK, Matheos D, Rose MD (1999). The cortical localization of the microtubule orientation protein, Kar9p, is dependent upon actin and proteins required for polarization. J Cell Biol 144, 963–975.

Moseley JB, Goode BL (2005). Differential activities and regulation of *Saccharomyces cerevisiae* formin proteins Bni1 and Bnr1 by Bud6. J Biol Chem 280, 28023–28033.

Moseley JB, Sagot I, Manning AL, Xu Y, Eck MJ, Pellman D, Goode BL (2004). A conserved mechanism for Bni1- and mDia1-induced actin assembly and dual regulation of Bni1 by Bud6 and profilin. Mol Biol Cell 15, 896–907.

Muhua L, Karpova TS, Cooper JA (1994). A yeast actin-related protein homologous to that in vertebrate dynactin complex is important for spindle orientation and nuclear migration. Cell 78, 669–679.

Nezami AG, Poy F, Eck MJ (2006). Structure of the autoinhibitory switch in formin mDia1. Structure 14, 257–263.

Otomo T, Otomo C, Tomchick DR, Machius M, Rosen MK (2005). Structural basis of Rho GTPase-mediated activation of the formin mDia1. Mol Cell 18, 273–281.

Ozaki-Kuroda K, Yamamoto Y, Nohara H, Kinoshita M, Fujiwara T, Irie K, Takai Y (2001). Dynamic localization and function of Bni1p at the sites of directed growth in *Saccharomyces cerevisiae*. Mol Cell Biol 21, 827–839.

Pruyne D, Evangelista M, Yang C, Bi E, Zigmond S, Bretscher A, Boone C (2002). Role of formins in actin assembly: nucleation and barbed-end association. Science 297, 612–615.

Pruyne D, Gao L, Bi E, Bretscher A (2004a). Stable and dynamic axes of polarity use distinct formin isoforms in budding yeast. Mol Biol Cell 15, 4971–4989.

Pruyne D, Legesse-Miller A, Gao L, Dong Y, Bretscher A (2004b). Mechanisms of polarized growth and organelle segregation in yeast. Annu Rev Cell Dev Biol 20, 559–591.

Rose R, Weyand M, Lammers M, Ishizaki T, Ahmadian MR, Wittinghofer A (2005). Structural and mechanistic insights into the interaction between Rho and mammalian Dia. Nature 435, 513–518.

Sagot I, Rodal AA, Moseley J, Goode BL, Pellman D (2002). An actin nucleation mechanism mediated by Bni1 and profilin. Nat Cell Biol 4, 626–631.

Santiago-Tirado FH, Legesse-Miller A, Schott D, Bretscher A (2011). PI4P and Rab inputs collaborate in myosin-V-dependent transport of secretory compartments in yeast. Dev Cell 20, 47–59.

Schroer TA (2004). Dynactin. Annu Rev Cell Dev Biol 20, 759–779.

Schumacher MA, Goodman RH, Brennan RG (2000). The structure of a CREB bZIP.somatostatin CRE complex reveals the basis for selective dimerization and divalent cation-enhanced DNA binding. J Biol Chem 275, 35242–35247.

Seth A, Otomo C, Rosen MK (2006). Autoinhibition regulates cellular localization and actin assembly activity of the diaphanous-related formins FRLalpha and mDia1. J Cell Biol 174, 701–713.
Sherman F (1991). Getting started with yeast. Methods Enzymol 194, 3–21.
Sheu YJ, Santos B, Fortin N, Costigan C, Snyder M (1998). Spa2p interacts with cell polarity proteins and signaling components involved in yeast cell morphogenesis. Mol Cell Biol 18, 4053–4069.
Shih JL, Reck-Peterson SL, Newitt R, Mooseker MS, Aebersold R, Herskowitz I (2005). Cell polarity protein Spa2P associates with proteins involved in actin function in *Saccharomyces cerevisiae*. Mol Biol Cell 16, 4595–4608.
Theesfeld CL, Irazoqui JE, Bloom K, Lew DJ (1999). The role of actin in spindle orientation changes during the *Saccharomyces cerevisiae* cell cycle. J Cell Biol 146, 1019–1032.
Tong AH *et al*. (2001). Systematic genetic analysis with ordered arrays of yeast deletion mutants. Science 294, 2364–2368.
Vallen EA, Caviston J, Bi E (2000). Roles of Hof1p, Bni1p, Bnr1p, and myo1p in cytokinesis in *Saccharomyces cerevisiae*. Mol Biol Cell 11, 593–611.
Wang J, Neo SP, Cai M (2009). Regulation of the yeast formin Bni1p by the actin-regulating kinase Prk1p. Traffic 10, 528–535.
Xu Y, Moseley JB, Sagot I, Poy F, Pellman D, Goode BL, Eck MJ (2004). Crystal structures of a formin homology-2 domain reveal a tethered dimer architecture. Cell 116, 711–723.
Yeh E, Yang C, Chin E, Maddox P, Salmon ED, Lew DJ, Bloom K (2000). Dynamic positioning of mitotic spindles in yeast: role of microtubule motors and cortical determinants. Mol Biol Cell 11, 3949–3961.
Yin H, Pruyne D, Huffaker TC, Bretscher A (2000). Myosin V orientates the mitotic spindle in yeast. Nature 406, 1013–1015.